Optics Letters

Diamond optical vortex generator processed by ultraviolet femtosecond laser

Si Gao,[1] Ze-Zheng Li,[1] Zhi-Yong Hu,[1] Feng Yu,[1] Qi-Dai Chen,[1] Zhen-Nan Tian,[1,3] and Hong-Bo Sun[1,2,4]

[1]State Key Laboratory of Integrated Optoelectronics, College of Electronic Science and Engineering, Jilin University, Changchun 130012, China
[2]State Key Laboratory of Precision Measurement Technology and Instruments, Department of Precision Instrument, Tsinghua University, Haidian, Beijing 100084, China
[3]e-mail: zhennan_tian@jlu.edu.cn
[4]e-mail:hbsun@tsinghua.edu.cn

Received 27 February 2020; revised 9 April 2020; accepted 13 April 2020; posted 13 April 2020 (Doc. ID 391598); published 1 May 2020

We propose a precise diamond micromachining method based on ultraviolet femtosecond laser direct writing and a mixed acid heating chemical treatment. The chemical composition of the attached clusters generated during laser ablation and their effects on morphologies were investigated in experiments. The averaged roughness of pristine and processed regions reduced to 0.64 nm and 9.4 nm from 20.5 nm and 37.4 nm, respectively. With this method, spiral zone plates (SZPs) were inscribed on a high-pressure high-temperature diamond surface as micro-optical vortex generators. The optical performances of the diamond SZPs were characterized in both experiments and simulations, which were very consistent with each other. This chemical auxiliary processing method will contribute greatly to the wide application of integration and miniaturization of diamond surface optical components.

https://doi.org/10.1364/OL.391598

With ultra-high hardness, large band-gap, good thermal stability, and unique optical properties, diamond can be used widely, ranging from precision cutting [1] and optical windows [2] to quantum platforms [3]. However, due to the high hardness and chemical stability, diamond is very difficult to process arbitrarily, which has always been the limitation of its wider application. At present, traditional methods to process diamond are usually mechanical polishing [4], dry etching [5], laser cutting [6], and so on [7]. However, mechanical polishing has low production efficiency and is limited to structures with large curvature radii, while dry etching technology is faced with expensive equipment, complex manual operations, and a strict reaction environment. The precision and roughness of traditional laser cutting have difficulty meeting the application requirements. Therefore, researchers are looking for new micro–nano machining methods to precisely process diamond. Ion beam etching (IBE) [8], inductively coupled plasma (ICP) [9], reactive ion etching (RIE) [10], and some other dry etching technologies are also developing rapidly. For example, recently, Hicks *et al*. presented a new cyclic Ar/O_2-Ar/Cl_2 ICP RIE process using an aluminum mask, with high-quality smooth features up to 10.6 μm with 0.47 nm surface roughness and 16.9:1 selectivity [11]. Furthermore, Xie *et al*. presented an ICP etching method that could expose certain crystal planes in monocrystalline diamond via changing the relevant etching factors. Also, diamond nanopillars with the largest tapering angle of 42 deg were presented, which could be used in nitrogen vacancy (NV) color center magnetometry and greatly help the NVs' high collection efficiency [12].

Nowadays, femtosecond laser direct writing technology has been utilized as a powerful tool to actualize three-dimensional (3D) structures with micro or sub-micro scales due to its advantages of high accuracy, real 3D ability, being mask-free, and having low cost [13–15]. For example, selectively erasing the second-order nonlinear optical coefficient, modulated in 3D space, was successfully realized by focusing a femtosecond laser inside lithium niobate crystal for the first time by Wei *et al*. [16]. So, it comes naturally that the femtosecond laser is used for diamond precision machining. In 2015, planar refractive lenses of 1 mm aperture and 500 μm parabola apex radii were realized on chemical vapor deposition (CVD) single-crystal diamond plates with a thickness of 300 μm by laser machining [17]. In 2016, 3D waveguides in diamond with high-quality NVs written by a femtosecond laser were presented, making them promising for integrated diamond chips used in quantum information fields [18]. However, in the process of femtosecond laser ablation on a diamond surface, it is difficult to remove the accumulated graphitized clusters without affecting the desired structures, which influences the machining accuracy and becomes the main factor limiting the application of femtosecond laser processing of diamond.

Here, we report ultraviolet (UV) femtosecond laser direct writing assisted by a mixed acid heating chemical treatment method to perform precise ablation on a diamond surface. The graphitized clusters, generated in the process of UV laser ablation on a high-pressure high-temperature (HPHT) diamond surface can be removed in the mixed acid of concentrated sulfuric acid and nitric acid heated to 80°C. With this method, the surface averaged roughness (Ra) reduced to 9.4 nm from 37.4 nm in the processed area. As a demonstration, optical

vortex generators were processed and showed good optical properties. The femtosecond laser ablation with chemical treatment method will be used for precise removal of accumulated graphitized clusters on a diamond surface and enhancing the potential of micro-, nano-structured diamond surface applications.

Compared with an infrared femtosecond laser, the UV femtosecond laser is more suitable for processing crystalline materials with large band gaps, such as sapphire and diamond [19]. In addition, in optical diffraction limitation theory, a shorter wavelength laser possesses higher processing accuracy in principle. In our experiment, an UV laser with wavelength of 343 nm generated by an integrated triple frequency module of Pharos (Light Conversion Ltd., Vilnius, Lithuania) fs-laser amplifier was used, whose pulse width and repetition rate were 230 fs and 200 kHz, respectively. The relative movement of the laser focus and HPHT diamond was precisely controlled by a commonly used laser scanning system consisting of two galvano-mirrors and a piezo-stage. Finally, the laser was focused on a diamond surface by an objective lens (Nikon, 20×, NA = 0.75), whose pulse energy was 55 nJ, measured in front of the objective. As shown in Fig. 1, the "OPTICS" letters, Jilin University's emblem, and a diffractive optical element [spiral zone plate (SZP)] were inscribed on diamond, which demonstrated the design flexibility. After laser processing, the sample was ultrasonic cleaned in acetone, ethanol, and deionized water for 15 min in turn. The optical microscope images (LEXT OLS4100, Olympus Corporation, Japan) of ablation patterns after ultrasonic cleaning without chemical treatment are shown in Figs. 1(a1)–1(c1). Then, the sample was treated by chemical treatment in mixed acid of concentrated sulfuric acid and nitric acid with a volume ratio of 8:1 for different durations [20]. Compared with Brown's recent work [21], this process can be accomplished without a complex distillation apparatus setup or high boiling temperatures (~200°C). The treatment durations of Figs. 1(a2)–1(c2), 1(a3)–1(c3), and 1(a4)–1(c4) were 10 min, 25 min, and 60 min, respectively. In Figs. 1(a1)–1(a4), with an increase in treatment time, the black matter around the letters disappeared, and the letters became clearer, obviously. Compared with Figs. 1(b1) and 1(b4), 1(c1) and 1(c4), after 1-h chemical treatment, the regions with laser scanning became much cleaner. The tightly attached clusters generated in the laser ablation process could not be removed by common ultrasonic cleaning. However, through a chemical heating treatment, these clusters were removed.

In order to confirm what kind of material was removed during the chemical treatment process, μ-Raman spectroscopy was carried out with the LabRAM HR Evolution instrument (HORIBA Ltd., Kyoto, Japan). A 532 nm He–Ne laser was used as the excitation source and focused by a 50× Olympus objective (NA = 0.5) on the laser ablation regions. Figure 2 shows the measurement results. The insets in Figs. 2(a) and 2(b) are SEM images of lines inscribed on a diamond surface by the UV laser before and after chemical treatment, and it is clear that the attached material disappears after chemical treatment. The pristine diamond surface has only a sp^3 characteristic peak at around 1332 cm^{-1}, as shown in the blue line in Fig. 2. After laser processing and ultrasonic cleaning, the G-peak at around 1575 cm^{-1} can be seen clearly, shown with a red line indicated by the black arrow. The cause of the G-peak is the in-plane stretching vibration of the sp^2 hybrid carbon atom, which indicates that the phase transition that took place in the laser scanning area was caused by graphitization of the diamond surface [22]. The test was repeated again after a 6-h chemical treatment. It is found that the G-peak disappears as the green line shows, and the Raman scattering peak near 1450 cm^{-1} is caused by the stretching vibration and bending vibration of C = C bond [23]. Hence, a convincing conclusion can be given that in the laser machining process, graphitized clusters are generated in the interaction between the laser focus and diamond surface, which cannot be removed by conventional acetone-ethanol-water ultrasonic cleaning, but can be thoroughly removed by chemical treatment.

Further morphology characterizations of the processed diamond surface before and after chemical treatment were investigated based on atomic force microscopy (AFM, Bruker Corporation, Dimension Icon). Figure 3 shows the AFM test results of the SZP structure with a topological charge of two before and after an 8-h chemical treatment. In Fig. 3, it can

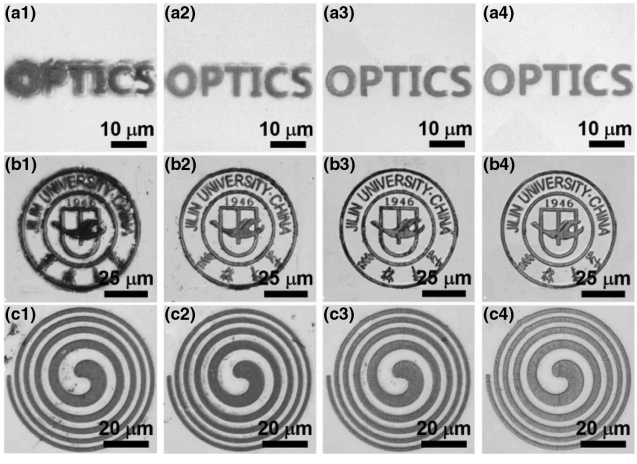

Fig. 1. Optical images of the patterns inscribed by ultraviolet laser on diamond surface vary with the increase in chemical treatment time. (a1)–(a4) "OPTICS" letters, (b1)–(b4) Jilin University's emblem, and (c1)–(c4) a diffractive optical element. (a1)–(c1) before chemical treatment, (a2)–(c2) treatment time = 10 min, (a3)–(c3) treatment time = 25 min, and (a4)–(c4) treatment time = 60 min.

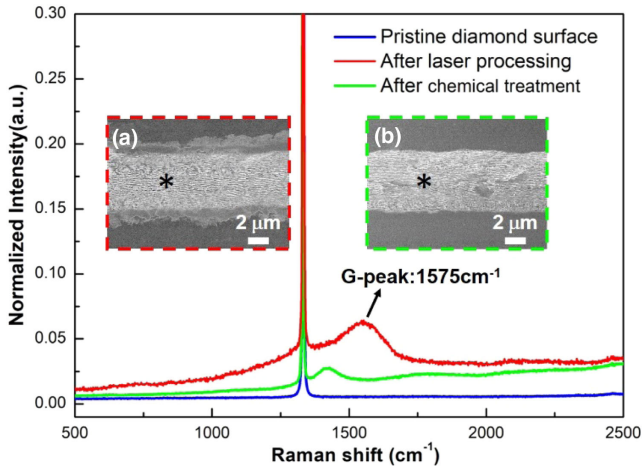

Fig. 2. μ-Raman spectroscopy of pristine diamond surface and regions after laser processing and after chemical treatment. Insets: (a), (b) SEM images of lines inscribed on diamond surface by UV laser before and after 6-h chemical treatment, respectively. The two black "*" in (a) and (b) indicate the testing positions.

be seen that large amounts of graphitized clusters are attached to the SZP structure before chemical treatment [(a1), (b1)], and disappear after chemical treatment [(a2), (b2)]. The Ra, a common feature parameter [24], of pristine and processed regions was investigated before and after chemical treatment. In Figs. 3(a1) and 3(a2), the central part of SZP, the Ra of the pristine and processed regions, highlighted with red and blue squares, reduced from 20.5 nm and 37.4 nm to 0.64 nm and 9.4 nm over $3 \times 3\ \mu m^2$ after chemical treatment, respectively. At the edge of SZP, 10 μm cross-section profiles of pristine and processed regions marked with red and blue dashed lines were extracted and are shown in Figs. 3(b1) and 3(b2). For the pristine region, the range of the cross-section curve reduced from ∼70 nm to ∼7 nm, which proved that the attached graphitized clusters were completely removed. For the processed region, the curve range reduced from ∼120 nm to ∼55 nm. The chemical treatment process acts like mechanical polishing of the diamond surface in pristine regions, while in processed regions, it helps to remove the clusters that cannot be removed by common ultrasonic cleaning. Thus, it can be concluded that the chemical treatment process can obviously reduce the roughness of femtosecond laser ablation diamond surface in both pristine and processed regions.

The optical vortex (OV) is a special optical field with phase singularity and orbital angular momentum (OAM), which has attracted extensive attention in the fields of quantum information technology and micro–nano manipulation [25]. In recent years, OV generators and NV color centers have been combined to become OAM quantum light sources, which were processed on the surface and induced inside of diamond by femtosecond lasers. Here, as a demonstration, high-performance SZPs were

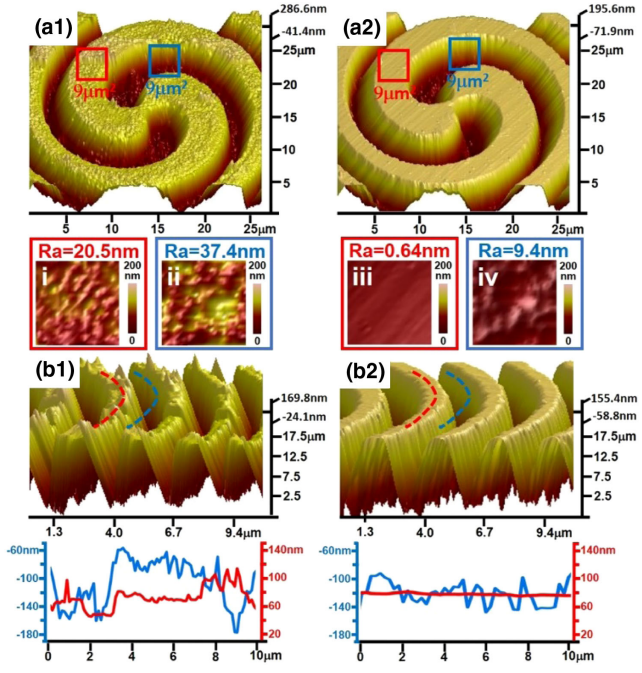

Fig. 3. AFM test results of the SZP structure with topological charge of two before [(a1), (b1)] and after [(a2), (b2)] 8-h chemical treatment. Red and blue squares mark the corresponding magnified areas in (a1), (a2). Cross-section curves in (b1), (b2) correspond to the pristine and processed positions marked with dashed red and blue lines, respectively.

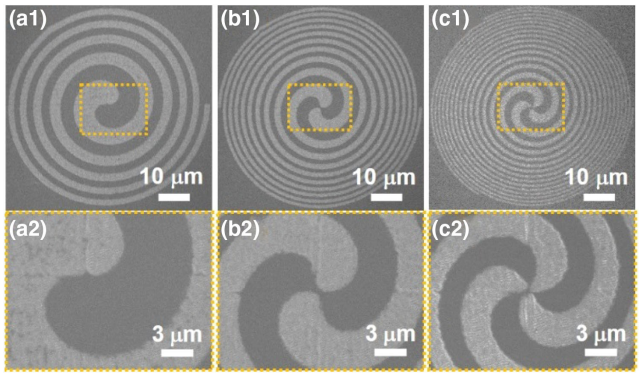

Fig. 4. SEM images of SZPs with different topological charges ($P = 1, 2, 3$) after 8-h chemical treatment to remove graphitized layer thoroughly. (a1) $P = 1$, (b1) $P = 2$, and (c1) $P = 3$; (a2)–(c2) correspond to detailed magnification areas marked with yellow dashed rectangles in (a1)–(c1).

processed as OV generators on a diamond surface by UV femtosecond laser direct writing assisted with a chemical treatment technique. The design of SZPs was achieved by phase addition and second-order quantization of a spiral phase plate (SPP) and Fresnel zone plate (FZP). After a lot of searching for the relevant laser parameters in the experiment, the processing single pulse energy of the femtosecond laser was optimized to 48.1 nJ prior to the objective lens, and the repetition frequency and scanning speed were 200 kHz and 2 mm/s, respectively. After laser processing, an 8-h chemical treatment of the sample was carried out.

Figures 4(a1)–4(c1) show the scanning electron microscope images (SEM, JSM-7500F, JEOL Ltd., Tokyo, Japan) of SZPs with topological charges of one, two, and three, respectively. The SZPs' sizes and shapes are in good agreement with the designs, and the diameter errors are less than 1 μm. In Figs. 4(a2)–4(c2), enlarged views of Figs. 4(a1)–(c1), no attached graphitized clusters can be found in either processed or pristine areas. The boundary between processed and pristine areas is smooth without noticeable aliasing, and accurate size with a clean surface ensures their good optical performance.

The optical properties of the diamond SZPs were characterized in both theoretical simulations and experiments in Fig. 5. For theoretical simulations, a beam propagation method based on scalar diffraction theory was adopted. The complex amplitudes of the SZP were set to zero, while the other areas were set to one. For the experiment, a He–Ne laser was used as the light source and was incident on SZPs vertically. An objective (Olympus, 50×, NA = 0.75) and an industrial charge coupled device (CCD, Mai Shi Wei Ltd., Shenzhen, China) of 5.0 megapixels were used as the microscopic observation system. In the focal plane, the energy distribution is a hollow ring, whose diameter increases with the topological charge. Figures 5(a1)–5(a3) and 5(b1)–5(b3) show the theoretical and experimental focal spots, respectively. The energy distributions and diameters of hollow light rings of different topologically charged OV beams are consistent with each other in both theory and experiment. The interference patterns of the OV beam and spherical wave [26] are shown in Figs. 5(c1)–5(c3) and 5(d1)–5(d3), respectively. In the interference patterns, the spirals reflect OV's spiral wavefront on a specific plane perpendicular to the optical axis. As the topological charge increases, the number of spirals

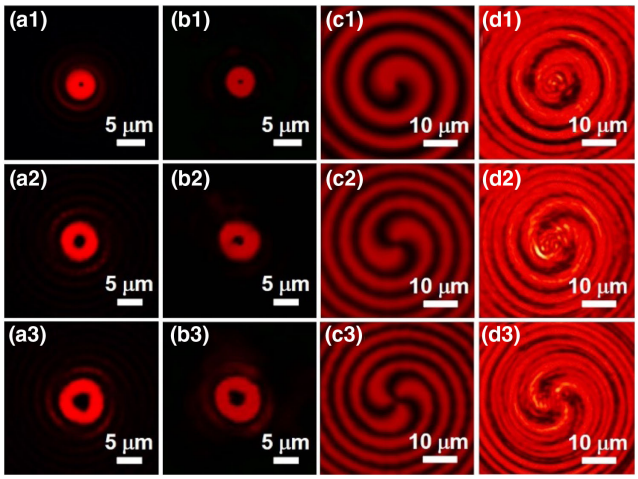

Fig. 5. Simulation and experimental results of focusing performances and interference patterns of SZPs with different topological charges: (a1)–(d1) $P = 1$, (a2)–(d2) $P = 2$, and (a3)–(d3) $P = 3$. (a1)–(a3) Simulation results of focusing performance and (b1)–(b3) corresponding test results. (c1)–(c3) Interference pattern simulation results and (d1)–(d3) their acquired patterns.

increases accordingly. The acquired patterns and theoretical simulation results are in good agreement. Further combined with single color centers in diamond, specially customized SZPs can be used as OAM quantum single photon sources. In addition, the diamond SZPs can work not only in visible light, but also in x-ray, which will greatly broaden the optical range of OV generators.

In summary, we report UV femtosecond laser direct writing assisted by a mixed acid heating chemical treatment method to achieve precise processing of diamond surface structures. After inscribing desired patterns on a diamond surface, the graphitized clusters were investigated and removed efficiently and thoroughly. The AFM characterization further verified the obvious reduction of surface roughness in pristine and processed areas, where Ra dropped from 20.5 nm to 0.64 nm and 37.4 nm to 9.4 nm over $3 \times 3\ \mu m^2$, respectively. As a demonstration, SZPs of different topological charges ($P = 1, 2, 3$) were prepared and showed good optical properties, and the experimental and theoretical simulation results of focusing performances with interference patterns were in good agreement. This work will provide a valuable reference for the subsequent fabrication of diamond surface optical elements, and the integration and miniaturization of optical elements using femtosecond laser machining.

Funding. National Basic Research Program of China (973 Program) (2017YFB1104600); National Natural Science Foundation of China (61825502, 61590930, 61827826, 61805098).

Disclosures. The authors declare no conflicts of interest.

REFERENCES

1. Z. F. Wang, J. J. Zhang, J. G. Zhang, G. Li, H. J. Zhang, H. ul Hassan, A. Hartmaier, Y. D. Yan, and T. Sun, J. Mater. Process. Technol. **276**, 116400 (2020).
2. A. Muhr and G. Mulligan, Photon. Spectra **50**, 46 (2016).
3. C. Bradac, W. B. Gao, J. Forneris, M. E. Trusheim, and I. Aharonovich, Nat. Commun. **10**, 5625 (2019).
4. H. Gong, S. J. Ao, K. T. Huang, Y. Wang, and C. Y. Yan, Nanotechnol. Precis. Eng. **2**, 118 (2019).
5. X. Q. Liu, Q. D. Chen, K. M. Guan, Z. C. Ma, Y. H. Yu, Q. K. Li, Z. N. Tian, and H. B. Sun, Laser Photon. Rev. **11**, 1600115 (2017).
6. D. Wyszynski, R. Ostrowski, M. Zwolak, and W. Bryk, AIP Conf. Proc. **1896**, 180007 (2017).
7. F. Lenzini, N. Gruhler, N. Walter, and W. H. P. Pernice, Adv. Quantum Technol. **1**, 1800061 (2018).
8. S. C. Mi, A. Toros, T. Graziosi, and N. Quack, Diam. Relat. Mater. **92**, 248 (2019).
9. X. Q. Liu, S. N. Yang, L. Yu, Q. D. Chen, Y. L. Zhang, and H. B. Sun, Adv. Funct. Mater. **29**, 1900037 (2019).
10. F. Gao, J. Van Erps, Z. Huang, H. Thienpont, R. G. Beausoleil, and N. Vermeulen, J. Phys. Photonics **1**, 015003 (2018).
11. M. L. Hicks, A. C. Pakpour-Tabrizi, and R. B. Jackman, Sci. Rep. **9**, 1 (2019).
12. L. Xie, T. X. Zhou, R. J. Stohr, and A. Yacoby, Adv. Mater. **30**, 1705501 (2018).
13. G. Chen, Z. Q. Wen, and C. W. Qiu, Light Sci. Appl. **8**, 56 (2019).
14. H. Wang, Y. L. Zhang, W. Wang, H. Ding, and H. B. Sun, Laser Photon. Rev. **11**, 1600116 (2017).
15. P. S. Salter and M. J. Booth, Light Sci. Appl. **8**, 110 (2019).
16. D. Z. Wei, C. W. Wang, H. J. Wang, X. P. Hu, D. Wei, X. Y. Fang, Y. Zhang, D. Wu, Y. L. Hu, J. W. Lie, S. N. Zhu, and M. Xiao, Nat. Photonics **12**, 596 (2018).
17. M. Polikarpov, I. Snigireva, J. Morse, V. Yunkin, S. Kuznetsov, and A. Snigirev, J. Synchrotron. Radiat. **22**, 23 (2015).
18. B. Sotillo, V. Bharadwaj, J. P. Hadden, M. Sakakura, A. Chiappini, T. T. Fernandez, S. Longhi, O. Jedrkiewicz, Y. Shimotsuma, L. Criante, R. Osellame, G. Galzerano, M. Ferrari, K. Miura, R. Ramponi, P. E. Barclay, and S. M. Eaton, Sci. Rep. **6**, 35566 (2016).
19. R. Srinivasan and V. Mayne-Banton, Appl. Phys. Lett. **41**, 576 (1982).
20. K. E. Carr, Carbon **8**, 155 (1970).
21. K. J. Brown, E. Chartier, E. M. Sweet, D. A. Hopper, and L. C. Bassett, J. Chem. Health Safety **26**, 40 (2019).
22. B. Sotillo, A. Chiappini, V. Bharadwaj, J. P. Hadden, F. Bosia, P. Olivero, M. Ferrari, R. Ramponi, P. E. Barclay, and S. M. Eaton, Appl. Phys. Lett. **112**, 031109 (2018).
23. A. C. Ferrari and J. Robertson, Phys. Rev. B **63**, 121405 (2001).
24. Y. Li, J. H. Yang, Z. J. Pan, and W. S. Tong, Fuel **260**, 116352 (2020).
25. Y. J. Shen, X. J. Wang, Z. W. Xie, C. J. Min, X. Fu, Q. Liu, M. L. Gong, and X. C. Yuan, Light Sci. Appl. **8**, 90 (2019).
26. M. S. Soskin, V. N. Gorshkov, M. V. Vasnetsov, J. T. Malos, and N. R. Heckenberg, Phys. Rev. A **56**, 4064 (1997).